AIAA JOURNAL
Vol. 42, No. 8, August 2004

Direct Approach in Inverse Problems for Dynamic Systems

Ki-Ook Kim,* Jin Yeon Cho,† and Young-Jae Choi‡
Inha University, Incheon 402-751, Republic of Korea

A direct and effective approach is presented for the inverse problem of dynamic structural systems, which is related to structural optimization, system identification, and damage detection. The structural modifications are sought for the characteristic changes assigned from the design goals or modal measurements. A finite element method is used for the system analysis and inverse problem. Mathematical programming techniques are applied for the minimization of the deviation of the finite element model from the desired inverse system, along with an objective function of least structural change. The modal method is based on the perturbation equations of a set of selected degrees of freedom and the energy equation associated with the frequency change. The mode shape change is expressed as the sum of the baseline mode shape and complementary vector, which plays a very important role in the search for the inverse solution. The linear perturbation equation is employed to get an initial approximation, which can be improved through iterations with the nonlinear perturbation equation. The proposed method does not involve the system reduction. Therefore, it is believed to be superior to conventional methods, which suffer from the residual error due to transformation of the eigenproblem.

Nomenclature

$\{A\}_j$, $\{A_p\}_j$	=	coefficient vectors for α_j, original and primary
$\{B\}$, $\{B_p\}$	=	constant vectors, original and primary
$\{C\}$, $\{C_p\}$	=	constant vectors, original and primary
c	=	self-contribution factor
$[D]$, $[D_{n-1}]$	=	dynamic stiffness matrices, original and partitioned
J	=	number of structural variables
$[k]$, $[k']$	=	stiffness matrices, baseline and perturbed
L	=	number of modes
$[m]$, $[m']$	=	mass matrices, baseline and perturbed
n	=	dimension of baseline system
$\{S\}$, $\{S_{n-1}\}$	=	constant vectors, original and partitioned
$\{T\}_j$, $\{T_{n-1}\}_j$	=	coefficient vectors for α_j, original and partitioned
$\alpha_1, \ldots, \alpha_J$	=	structural variables
α_j^L, α_j^U	=	lower and upper bounds for α_j
$[\Delta k]$, $[\Delta k]_j$	=	stiffness changes for system and α_j
$[\Delta m]$, $[\Delta m]_j$	=	mass changes for system and α_j
$\Delta\lambda$	=	eigenvalue change
$\{\Delta\phi\}$	=	mode shape change
λ, λ'	=	eigenvalues, baseline and perturbed
$\{\phi\}$, $\{\phi'\}$	=	mode shapes, baseline and perturbed
$\{\phi_p\}$, $\{\phi_s\}$	=	primary and secondary sets
ϕ_r, $\Delta\phi_r$	=	reference degree of freedom and its change
$\{\psi\}$, $\{\psi_p\}$	=	complementary vector, original and primary

Subscript

app	=	approximation

Introduction

EVER-INCREASING capabilities of digital computers have enabled finite element theories to serve as a practical tool for the analysis and synthesis of complicated structures. Continuous structural properties such as stiffness and mass are discretized to yield a finite element model, which is used to obtain the desired static and dynamic responses of the structural system.

When the structural analysis indicates undesirable characteristics, it is not easy to know where and how much the baseline system should be modified to achieve the desired goals. In structural optimization,[1–3] equilibrium equations of the perturbed system can be combined with mathematical programming techniques to get an optimum design.

Although the finite element analysis is usually accurate enough to describe the structural behavior of the real system, modeling errors from various sources can arouse a serious question about the credibility of the finite element solution. Then, the finite element model is updated, so that the numerical solution may get closer to the test results. The procedure of system identification or model updating[4–6] adjusts the inherent mismatch between the analytical and real systems, that is, it validates the finite element model by the use of the measured data of the system characteristics. Computer simulations with the updated model can provide the structural responses that cannot be obtained through practical engineering tests.

In recent years, increasing attention has been focused on structural health monitoring and damage detection[7–9] in aerospace, nuclear, and civil engineering fields. Periodic tests and measurements are carried out to check the probability of structural failure. Detection of the structural damage reveals both the location and extent of the element changes in the system. For a general discussion, readers are referred to the comprehensive research works of Friswell and Mottershead,[10] Friswell et al.,[11] and Penny et al.,[12] which have motivated the present study.

In the inverse problem of structural optimization, system identification, and damage detection, the baseline structure is modified to get a perturbed system that gives the specified static and dynamic characteristics. In structural optimization, an optimum design is selected from many feasible solutions, whereas a unique structure must be determined in damage detection. On the other hand, the system identification may yield a single or several inverse systems that can be used for structural simulations.

A common approach to inverse problems is the modal method, in which the changes in modal characteristics (natural frequencies and mode shapes) are related to the modifications of the structural properties (stiffness and mass). In practice, various problems are encountered in the theoretical formulation as well as engineering measurement.

As is well known, the accuracy of eigenvalue is of the second order when eigenvector differs from the exact value by a small quantity of the first order.[13] In typical measurements for natural frequency and mode shape, about 0.1 and 10% errors were observed.[14] Hence,

Received 27 February 2003; revision received 28 November 2003; accepted for publication 13 March 2004.

*Professor, Aerospace Engineering. Senior Member AIAA.
†Assistant Professor, Aerospace Engineering.
‡Doctoral Student, Aerospace Engineering; currently Senior Researcher, Department of Aviation Safety, Korea Transportation Safety Authority, 523 Gojandong, Ansan Kyunggido 425-801, Republic of Korea.

natural frequencies (eigenvalues) are preferred over mode shapes for the modal data.

A minor problem occurs in that the energy equation associated with the eigenvalue is only a necessary condition for the system equilibrium and, hence, cannot provide sufficient information for the inverse solution.[15] In addition, the energy of an eigenmode is the sum of energies of all elements (or degrees of freedom) and, thus, the effects of an element change are spread over the entire structure. Hence, natural frequencies become less sensitive to element changes.

Another problem comes from the fact that all degrees of freedom cannot be given in mode shapes. In structural optimization, major components are specified as desired and others are free to drift. In system identification and damage detection, a limited number of sensors are placed on the measurable degrees of freedom at the accessible nodes of the real structure.

Therefore, primary (master) degrees of freedom are given in the formulation, and secondary (slave) ones are omitted. The transformation between the primary and secondary sets is conducted with the structural matrices (physical approach)[16–19] or mode shapes (mathematical approach).[20,21] Through the system transformation, the equilibrium equation is approximated in terms of the primary set, which represents the eigenvector of the reduced eigenproblem.

In the present study, only the equilibrium equations of the primary degrees of freedom are employed, along with the energy equation related to the eigenvalue change. Because the dynamic stiffness matrix is singular, the mode shape change is expressed as the sum of the baseline mode and a complementary vector, which plays an important role for the inverse solution.

Mathematical programming techniques are applied for the minimization of the deviation of the finite element model from the desired inverse system. The objective function of least structural change tends to distribute the element changes over the entire structure, which may be desirable in optimization but rather misleading in the search for a unique solution.

The proposed method does not involve system reductions and, hence, is not subject to the residual error due to system transformation. The linear perturbation equation gives a good approximation, which can be improved through iterations with the nonlinear equation.

Inclusion of more modes shows an overall tendency of steady, if not uniform, convergence of the inverse solution. Sometimes, the primary degrees of freedom of the added modes may be linearly dependent to some extent and, hence, give a minor improvement. Normalization of the energy equations by eigenvalues is recommended to accelerate the convergence.

The sensitivities of the characteristic variables are much larger than those of the structural variables, causing small errors in measurement to bring excessive structural modifications. Further research is required to explore numerical instability of the perturbed system.

Problem Formulation

In finite element dynamic analysis, the equilibrium equation of undamped free vibration is written as a general eigenproblem:

$$[k]\{\phi\} = \lambda[m]\{\phi\} \tag{1}$$

where $[k]$ and $[m]$ are the stiffness and mass matrices. An eigenpair is given as λ and $\{\phi\}$.

Modifications of the baseline structure yield a perturbed system,

$$[k']\{\phi'\} = \lambda'[m']\{\phi'\} \tag{2}$$

that can be expressed in terms of perturbations as

$$([k] + [\Delta k])(\{\phi\} + \{\Delta\phi\}) = (\lambda + \Delta\lambda)([m] + [\Delta m])(\{\phi\} + \{\Delta\phi\}) \tag{3}$$

The nonlinear perturbation equation has terms up to third order in perturbation.

In the forward perturbation, for reanalysis and design sensitivity analysis, the characteristic changes $\Delta\lambda$ and $\{\Delta\phi\}$ are calculated from the structural modifications $[\Delta k]$ and $[\Delta m]$. The procedure is straightforward, and the solution is unique.

In inverse problems, however, the perturbed structure of $[k']$ and $[m']$ is sought to get the desired modal characteristics λ' and $\{\phi'\}$. In structural optimization, there may exist many feasible systems that give the specified characteristic changes. Then, an objective function of minimum weight or least change is assigned to get an optimum solution. On the other hand, a single inverse system must be uniquely determined in system identification and damage detection. Hence, the problem usually becomes overdetermined.

A practical question is what and how much information should be provided to calculate the correct structural changes, accurately and efficiently. The more modes and degrees of freedom are included, the better solution can be obtained through an increased computational effort. The information needs to be linearly independent to minimize the redundancy.

The nonlinear perturbation equation (3) can be rearranged to get

$$\begin{aligned}([k] - \lambda[m])\{\Delta\phi\} &= -([\Delta k] - \lambda[\Delta m])(\{\phi\} + \{\Delta\phi\}) \\ &\quad + \Delta\lambda([m] + [\Delta m])(\{\phi\} + \{\Delta\phi\})\end{aligned} \tag{4}$$

Assuming that the structural modifications and the consequent characteristic changes are small, one obtains the linear perturbation equation

$$([k] - \lambda[m])\{\Delta\phi\} = -([\Delta k] - \lambda[\Delta m])\{\phi\} + \Delta\lambda[m]\{\phi\} \tag{5}$$

The structural perturbations are decomposed into the contributions of J structural variables:

$$\begin{aligned}[\Delta k] &= [\Delta k]_1 + \cdots + [\Delta k]_J = \sum_{j=1}^{J} [\Delta k]_j \\ [\Delta m] &= [\Delta m]_1 + \cdots + [\Delta m]_J = \sum_{j=1}^{J} [\Delta m]_j\end{aligned} \tag{6}$$

where $[\Delta k]_j$ and $[\Delta m]_j$ are linear or nonlinear functions of the structural variable α_j.

Substituting Eq. (6) into Eq. (5), one gets

$$([k] - \lambda[m])\{\Delta\phi\} = -\{T\}_1 - \cdots - \{T\}_J + \{S\} \tag{7}$$

where

$$\begin{aligned}\{T\}_j &= ([\Delta k]_j - \lambda[\Delta m]_j)\{\phi\}, \qquad j = 1, \ldots, J \\ \{S\} &= \Delta\lambda[m]\{\phi\}\end{aligned} \tag{8}$$

Note that the vector $\{T\}_j$ contains the structural variable α_j.

The equilibrium equation (1) of the baseline system can be rewritten as

$$([k] - \lambda[m])\{\phi\} = \{0\} \tag{9}$$

From Eqs. (7) and (9), it can easily be seen that an arbitrary combination of $\{\phi\}$ with $\{\Delta\phi\}$ satisfies the perturbation equation (7). Hence, a complementary vector $\{\psi\}$ is introduced as

$$\{\Delta\phi\} = \{\psi\} + c\{\phi\} \tag{10}$$

where the self-contribution factor c is determined according to the mode normalization.

When mass normalization is employed for both $\{\phi\}$ and $\{\phi'\}$, we have

$$\{\phi\}^T[m]\{\phi\} = 1, \qquad \{\phi'\}^T[m']\{\phi'\} = 1 \tag{11}$$

If $\{\psi\}$ is orthogonal to $\{\phi\}$ with respect to $[m]$, the first-order perturbation equation of the mass normalization gives

$$c = -\tfrac{1}{2}\{\phi\}^T[\Delta m]\{\phi\} \tag{12}$$

In the current work, a reference degree of freedom is selected to have fixed magnitudes. Then, the reference components of $\{\phi\}$ and $\{\phi'\}$ are compared to obtain the change $\Delta\phi_r$:

$$\Delta\phi_r = \phi'_r - \phi_r \tag{13}$$

To remove the singularity of the dynamic stiffness matrix in the inverse calculation, the reference row and column are partitioned out and the corresponding component of $\{\psi\}$ is set to zero or $\psi_r = 0$. Then, Eq. (10) can be rewritten as

$$\{\Delta\phi\} = \begin{Bmatrix} \Delta\phi_{n-1} \\ \Delta\phi_r \end{Bmatrix} = \begin{Bmatrix} \psi_{n-1} \\ 0 \end{Bmatrix} + c \begin{Bmatrix} \phi_{n-1} \\ \phi_r \end{Bmatrix} \tag{14}$$

or

$$c = \Delta\phi_r / \phi_r \tag{15}$$

For simplicity, the largest component is often selected as the reference degree of freedom with unit magnitude. If structural modifications and consequent characteristic changes are small, no mode shift occurs, and we get $\phi'_r = \phi_r = 1$, $\Delta\phi_r = 0$, and $c = 0$.

On the other hand, substitution of Eq. (10) into Eq. (7) gives

$$[D]\{\psi\} = -\{T\}_1 - \cdots - \{T\}_J + \{S\} \tag{16}$$

Note that the dynamic stiffness matrix $[D] = [k] - \lambda[m]$ is singular.

For a distinct eigenvalue λ, the matrix $[D]$ has the rank of $n - 1$. Through partitioning out the reference row and column, we get a nonsingular matrix $[D_{n-1}]$. Elimination of the relevant rows from $\{\psi\}$, $\{T\}_j$, and $\{S\}$ in Eq. (16) gives $\{\psi_{n-1}\}$, $\{T_{n-1}\}_j$, and $\{S_{n-1}\}$:

$$[D_{n-1}]\{\psi_{n-1}\} = -\{T_{n-1}\}_1 - \cdots - \{T_{n-1}\}_J + \{S_{n-1}\} \tag{17}$$

Equation (17) can be solved to get

$$\{\psi_{n-1}\} = -\{A_{n-1}\}_1 - \cdots - \{A_{n-1}\}_J + \{C_{n-1}\} \tag{18}$$

where

$$\{A_{n-1}\}_j = [D_{n-1}]^{-1}\{T_{n-1}\}_j, \qquad j = 1, \ldots, J$$

$$\{C_{n-1}\} = [D_{n-1}]^{-1}\{S_{n-1}\} \tag{19}$$

As was mentioned before, the mode shape can be divided into primary and secondary parts:

$$\{\phi'\} = \begin{Bmatrix} \phi'_p \\ \phi'_s \end{Bmatrix} = \begin{Bmatrix} \phi_p \\ \phi_s \end{Bmatrix} + \begin{Bmatrix} \Delta\phi_p \\ \Delta\phi_s \end{Bmatrix} \tag{20}$$

The specified or measured degrees of freedom are included in the primary set $\{\phi'_p\}$ (or $\{\Delta\phi_p\}$). The secondary set $\{\phi'_s\}$ (or $\{\Delta\phi_s\}$) represents the free or unknown components.

In the same way, Eq. (10) can be written in partitioned form as

$$\begin{Bmatrix} \Delta\phi_p \\ \Delta\phi_s \end{Bmatrix} = \begin{Bmatrix} \psi_p \\ \psi_s \end{Bmatrix} + c \begin{Bmatrix} \phi_p \\ \phi_s \end{Bmatrix} \tag{21}$$

Because the modal data of $\{\Delta\phi_p\}$ is given, the primary set of $\{\psi\}$ is obtained as

$$\{\psi_p\} = \{\Delta\phi_p\} - c\{\phi_p\} \tag{22}$$

From Eq. (18), the equations for the primary degrees of freedom can be extracted as

$$\{\psi_p\} = -\{A_p\}_1 - \cdots - \{A_p\}_J + \{C_p\} \tag{23}$$

which is rearranged to get

$$\{A_p\}_1 + \cdots + \{A_p\}_J = \{C_p\} - \{\psi_p\} \equiv \{B_p\} \tag{24}$$

The energy equation for the eigenvalue change can be used to secure the solution convergence. Premultiplication of Eq. (5) by $\{\phi\}^T$ gives

$$\{\phi\}^T([\Delta k] - \lambda[\Delta m])\{\phi\} = \Delta\lambda\{\phi\}^T[m]\{\phi\} \tag{25}$$

Substitution of Eq. (6) into Eq. (25) yields

$$\{\phi\}^T\{T\}_1 + \cdots + \{\phi\}^T\{T\}_J = \{\phi\}^T\{S\} \tag{26}$$

The left-hand sides of Eqs. (24) and (26) contain the structural variables $\alpha_1, \ldots, \alpha_J$, which are determined in the inverse solution. The equilibrium equations of the perturbed system are used as equality constraints in the mathematical programming techniques.

Iteration Procedures

Linear Perturbation Equation

The iteration procedure for the inverse solution starts from the linear perturbation equation (5). For an objective function of least structural change and the equality constraint equations (24) and (26), the mathematical programming problem is written as

$$F = \{\alpha\}^T\{\alpha\} = \alpha_1^2 + \cdots + \alpha_J^2$$

minimized, with constraints

$$\{A_p\}_1 + \cdots + \{A_p\}_J = \{B_p\}$$

$$\{\phi\}^T\{T\}_1 + \cdots + \{\phi\}^T\{T\}_J = \{\phi\}^T\{S\}$$

$$\alpha_j^L \le \alpha_j \le \alpha_j^U, \qquad j = 1, \ldots, J \tag{27}$$

Figure 1 shows the flow diagram of the solution procedure of linear perturbation equation. The stiffness and mass matrices, $[\Delta k]_j$ and $[\Delta m]_j$, are derived for each design variable α_j. The corresponding coefficient vectors, $\{T\}_j$ and $\{A_{n-1}\}_j$ are calculated for each mode. The primary set $\{A_p\}_j$ is selected from $\{A_{n-1}\}_j$.

The constant vectors $\{S\}$ and $\{C_{n-1}\}$ are calculated for each mode. The given primary data $\{\Delta\phi_p\}$ and $\{\phi_p\}$ are applied to get $\{\psi_p\}$. The primary set of $\{C_{n-1}\}$ is selected to obtain $\{C_p\}$, and the right-hand side of the equation $\{B_p\}$ is determined.

The energy equation for the eigenvalue change is added to improve the solution convergence. Normalization of the equations by the eigenvalues is recommended if significant changes are specified on eigenvalues. Side constraints may be assigned for the lower and upper bounds of the variables. The mathematical programming gives an approximation $\{\alpha\}_{\text{app}}$.

For the subsequent iteration with the nonlinear perturbation equation, $[m']$ and $\{\phi'\}$ are updated through system reanalysis. The element changes with $\{\alpha\}_{\text{app}}$ are added to get the structural modifications of the system, $[\Delta k]_{\text{app}}$ and $[\Delta m]_{\text{app}}$:

$$[\Delta k]_{\text{app}} = [\Delta k]_1 + \cdots + [\Delta k]_J$$

$$[\Delta m]_{\text{app}} = [\Delta m]_1 + \cdots + [\Delta m]_J \tag{28}$$

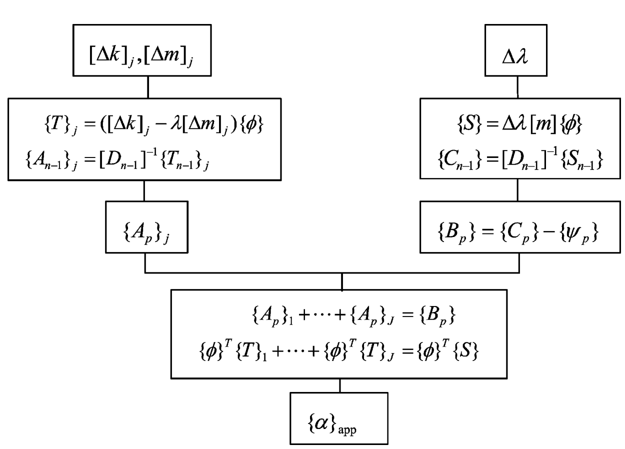

Fig. 1 Flow diagram of linear perturbation.

The structural perturbations are substituted into the linear perturbation equation, and the decomposed matrix of $[D_{n-1}]$ is employed to get $\{\psi_{n-1}\}_{\text{app}}$. The complementary vector $\{\psi\}_{\text{app}}$ is combined with the baseline mode shape $\{\phi\}$ to calculate $\{\Delta\phi\}_{\text{app}}$. Finally, one gets the updated mode shape $\{\phi'\}_{\text{app}}$ and mass matrix $[m']_{\text{app}}$, as shown in Fig. 2.

Nonlinear Perturbation Equation

The linear perturbation equation gives a good approximation, which can be improved through nonlinear iterations. The nonlinear perturbation equation (4) can be rewritten as

$$([k]-\lambda[m])\{\Delta\phi\} = -([\Delta k]-\lambda[\Delta m])\{\phi'\}_{\text{app}} + \Delta\lambda[m']_{\text{app}}\{\phi'\}_{\text{app}} \tag{29}$$

The problem of mathematical programming for nonlinear iterations is written as

$$F = \{\alpha\}^T\{\alpha\} = \alpha_1^2 + \cdots + \alpha_J^2$$

minimized, with constraints

$$\{A'_p\}_1 + \cdots + \{A'_p\}_J = \{B'_p\}$$

$$\{\phi\}^T\{T'\}_1 + \cdots + \{\phi\}^T\{T'\}_J = \{\phi\}^T\{S'\}$$

$$\alpha_j^L \le \alpha_j \le \alpha_j^U, \qquad j = 1, \ldots, J \tag{30}$$

Figure 3 shows the calculation procedure of nonlinear inverse solution. Note that the primary part of the complementary vector remains constant. The update of $\{\phi'\}$ and $[m']$ is shown in Fig. 4.

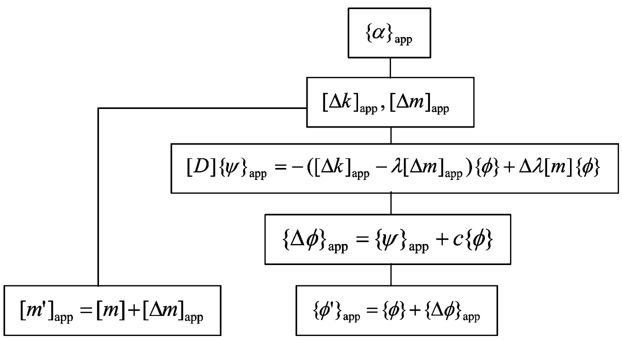

Fig. 2 Flow diagram of linear update.

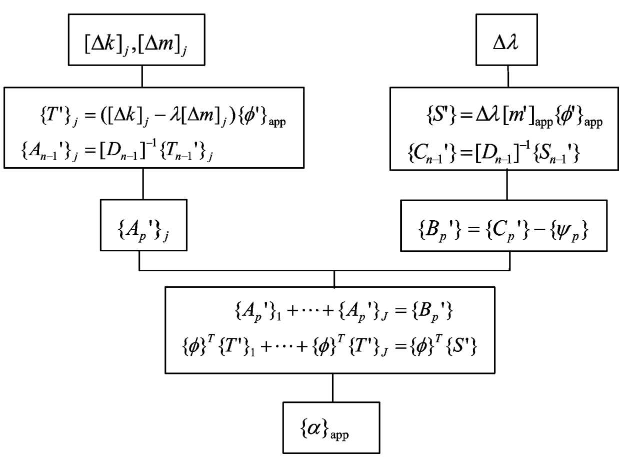

Fig. 3 Flow diagram of nonlinear perturbation.

Numerical Examples

Cantilever Beam

The flexural vibration of a cantilever beam[22] is used for the detectability and accuracy assessment of the proposed method. The finite element model has 15 small and 10 large beam elements, as shown in Fig. 5. The planar bending motion will be described by the use of the translational and rotational displacements of 25 unconstrained nodes. Hence, the structural system has 50 degrees of freedom.

For simplicity, the width b of the beam element was defined as the structural variable. Hence, the change of the design variable would affect both the mass and the stiffness of the system. The widths of four elements 5, 10, 19, and 25 were reduced, as shown in Fig. 6.

A finite element program was used to obtain the eigenvalues of the baseline and perturbed systems listed in Table 1. Note that even the significant element modifications do not cause noticeable changes in the eigenvalues, resulting in small design sensitivities.

The transverse displacement of the tip was selected as the reference degree of freedom. The exact modal data of the perturbed system were used for both the eigenvalues and the translational degrees of freedom of nine primary nodes, as shown in Fig. 7. The primary set[22] is known to be a good selection in the physical transformation.

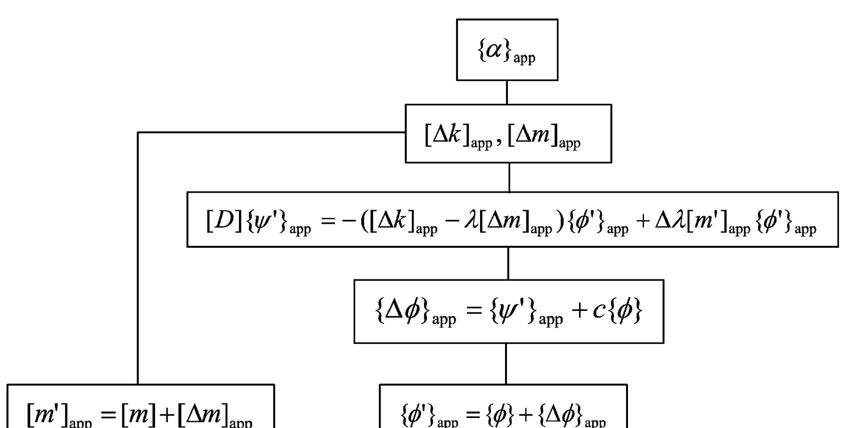

Fig. 4 Flow diagram of nonlinear update.

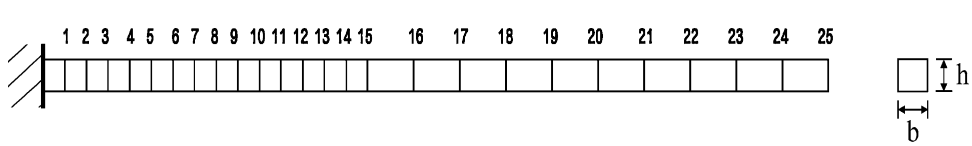

Fig. 5 Baseline beam in flexural vibration: $b = 40$ mm, $h = 40$ mm, $L = 3.5$ m, $E = 6.9 \times 10^4$ MPa, and $\rho = 2.7 \times 10^{-9}$ Ns^2/mm.[4]

Table 1 Eigenvalues of cantilever beams

Mode	Baseline	Perturbed	% change
1	2.80703×10^2	2.93392×10^2	+4.52
2	1.10244×10^4	1.14945×10^4	+4.26
3	8.64349×10^4	9.02208×10^4	+4.38
4	3.31948×10^5	3.47170×10^5	+4.59
5	9.07265×10^5	9.39662×10^5	+3.57

Table 2 Eigenvalue of inverse system (mode 1)

Mode 1	Value	% change
Perturbed	2.93392×10^2	+4.52
Inverse	2.93389×10^2	+4.52

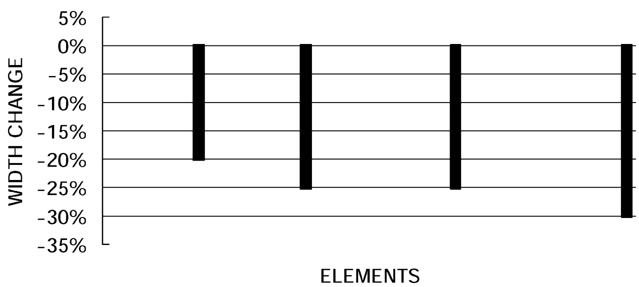

Fig. 6 Perturbed beam elements.

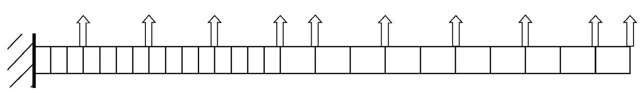

Fig. 7 Primary and reference nodes.

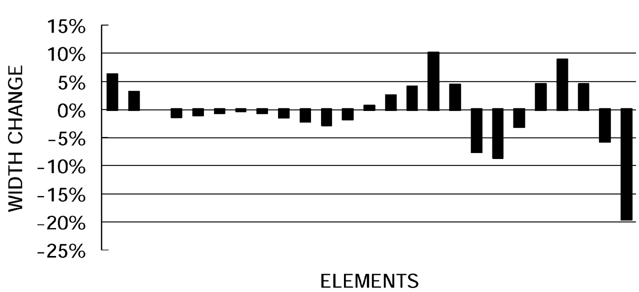

Fig. 8 Inverse solution (mode 1).

In five subcases, the number of modes was increased one by one to observe the overall detectability of the inverse solution. To examine the solution accuracy, the eigenvalues of the inverse systems were compared with those of the perturbed system.

A penalty function method was employed, and the convergence tolerance was set to 10% variation of the design variables, or $\|\{\Delta\alpha\}\|$. The objective function of least structural change would not only tend to spread the effects of an element change over the entire structure, but also prevent the design variables from jumping to excessive values in iterations.

In general, the first nonlinear iteration shows a considerable variation of the structural variables from the linear perturbation solution. Hence, two or more nonlinear iterations were carried out to stabilize the solutions.

Mode 1

The inverse problem has 10 equations for 25 variables and, hence, becomes underdetermined. The inverse solution of two nonlinear iterations gave the element changes in Fig. 8, which were far from the real perturbations in Fig. 6. The inverse system gives the eigenvalue in Table 2.

Table 3 Eigenvalues of inverse system (modes 1 and 2)

Mode	Perturbed	% change	Inverse	% change
1	2.93392×10^2	+4.52	2.93401×10^2	+4.52
2	1.14945×10^4	+4.26	1.14937×10^4	+4.26

Table 4 Eigenvalues of inverse system (modes 1–3)

Mode	Perturbed	% change	Inverse	% change
1	2.93392×10^2	+4.52	2.93361×10^2	+4.51
2	1.14945×10^4	+4.26	1.14944×10^4	+4.26
3	9.02208×10^4	+4.38	9.02173×10^4	+4.38

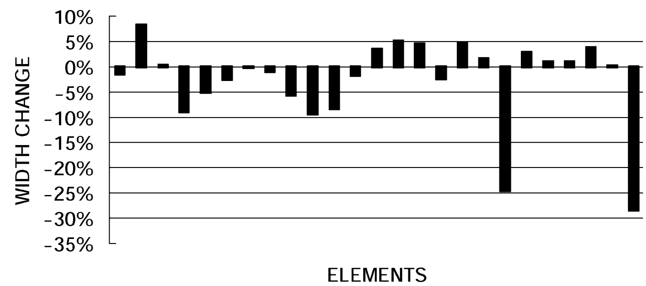

Fig. 9 Inverse solution (modes 1 and 2).

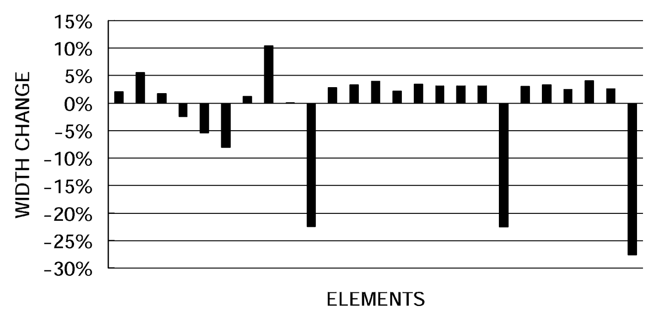

Fig. 10 Inverse solution (modes 1–3).

Modes 1 and 2

Inclusion of the second mode will double the number of equations to make 20, still resulting in an underdetermined problem. The element changes obtained after eight nonlinear iterations are shown in Fig. 9. Table 3 shows the eigenvalues of the inverse system.

Modes 1–3

When three modes are involved in the equation formulation, the inverse problem has 30 equations for 25 variables and, hence, becomes overdetermined. The inverse solution took nine nonlinear iterations to get the element changes shown in Fig. 10.

More correct element perturbations appear with minor disturbances, in particular, near the tip of the beam. The perturbed element 5, which is located near the wall and experiences small displacements, does not come out yet. The eigenvalues are illustrated in Table 4.

Modes 1–4

The element changes in Fig. 11 were obtained with nine nonlinear iterations. Still, the perturbed element 5 near the wall was hidden between the adjacent elements 4 and 6, whereas the other element perturbations were found correctly.

Inclusion of an additional mode does not always guarantee a uniform improvement in the solution if the primary modal data are somewhat linearly dependent on those of other modes. Nevertheless, the inverse procedure yields a slow but steady improvement in the detectability of the converged solution. The inverse system gives the accurate eigenvalues as shown in Table 5.

Table 5 Eigenvalues of inverse system (modes 1–4)

Mode	Perturbed	% change	Inverse	% change
1	2.93392×10^2	+4.52	2.93347×10^2	+4.50
2	1.14945×10^4	+4.26	1.14942×10^4	+4.26
3	9.02208×10^4	+4.38	9.02148×10^4	+4.37
4	3.47170×10^5	+4.59	3.47116×10^5	+4.57

Table 6 Eigenvalues of inverse system (modes 1–5)

Mode	Perturbed	% change	Inverse	% change
1	2.93392×10^2	+4.52	2.93552×10^2	+4.58
2	1.14945×10^4	+4.26	1.14958×10^4	+4.28
3	9.02208×10^4	+4.38	9.02386×10^4	+4.40
4	3.47170×10^5	+4.59	3.47235×10^5	+4.61
5	9.39662×10^5	+3.57	9.39783×10^5	+3.58

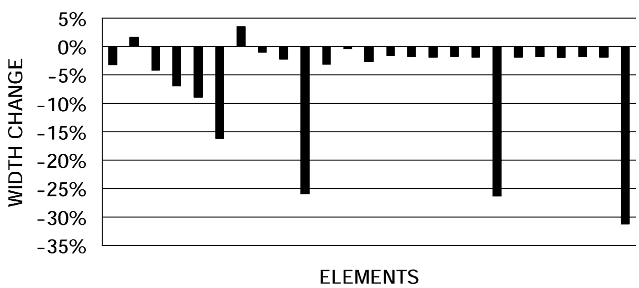

Fig. 11 Inverse solution (modes 1–4).

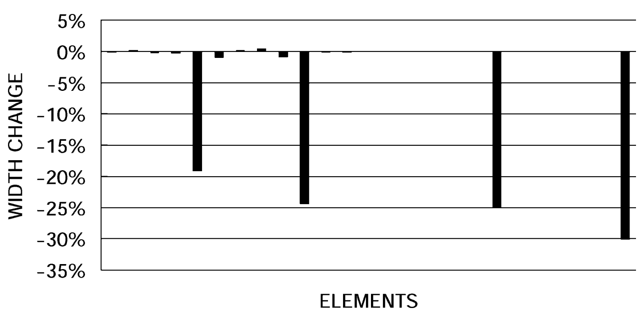

Fig. 12 Inverse solution (modes 1–5).

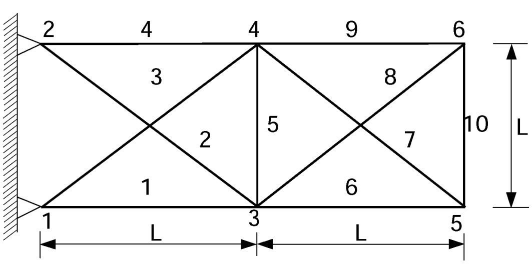

Fig. 13 Truss structure in planar motion: $A = 10$ mm × 10 mm, $L = 1$ m, $E = 6.9 \times 10^4$ MPa, and $\rho = 2.7 \times 10^{-9}$ Ns²/mm⁴.

Modes 1–5

The addition of fifth mode gave a drastic improvement for the inverse solution. A total of 14 nonlinear iterations were performed to get the perturbed elements correctly, as shown in Fig. 12. The reanalysis of the inverse system gives the eigenvalues in Table 6.

Truss Structure

Another numerical example is a truss structure of Fig. 13. The system has 6 nodes and 10 bar elements that carry only axial loads. With four unconstrained nodes moving in a planar motion, the system has eight translational degrees of freedom.

Table 7 Eigenvalues of truss structures

Mode	Baseline	Perturbed	% change
1	1.67661×10^6	1.61650×10^6	−3.59
2	1.18949×10^7	1.14531×10^7	−3.71
3	1.61529×10^7	1.49417×10^7	−7.50
4	5.18046×10^7	5.17365×10^7	−0.13
5	9.02966×10^7	8.33865×10^7	−7.65

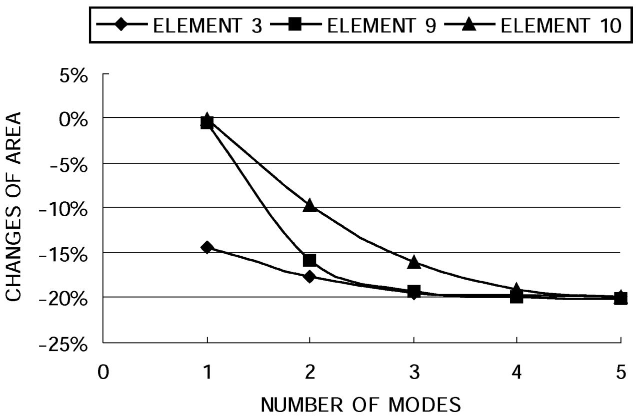

Fig. 14 Convergence of bar elements.

The cross-sectional areas of the elements are defined as the structural variables. In this case, only the element stiffness was allowed to change, whereas the mass remains constant. The cross-sectional areas of three elements, 3, 9, and 10, have been reduced by 20%. The eigenvalues of the baseline and perturbed systems are shown in Table 7.

The vertical displacement of node 6 is the reference degree of freedom. The primary set includes the vertical displacements of nodes 3, 4, and 5. For 10 structural variables, the inverse problem has four equations in each mode.

The same solution procedure was applied to get the inverse system. Figure 14 illustrates the perturbed elements converging to −20% as the number of modes increases to five.

As before, the number of modes was increased one by one in five subcases. The solution convergence was achieved with 8–13 nonlinear iterations. In all subcases, the inverse systems gave the accurate eigenvalues specified from the perturbed system.

Conclusions

An iterative method has been presented for the inverse problem of dynamic structural systems. The method is based on the equilibrium equations of a set of selected degrees of freedom and the energy equation associated with the frequency change. The mode shape change is expressed as a combination of the baseline mode shape and a complementary vector.

A penalty function method was employed, along with an objective function of least structural change. The linear perturbation equation gives a good approximation for iterations with the nonlinear perturbation equation. The incremental change of the structural variables is used for the convergence criterion.

As more modes are involved in the formulation, the inverse problem becomes highly overdetermined. In practice, however, the primary modal data may be redundant or linearly dependent to some extent. Inclusion of additional modes gives a steady, if not uniform, improvement in the detectability of the inverse solution. The reanalysis of the inverse systems shows the exact modal characteristics specified from the perturbed system.

Normalization of the energy equations with eigenvalues is recommended when many modes are employed in inverse problems. It was found that errors in the modal data had significant effects on the accuracy of the inverse solution. Further research work is under way to secure the numerical stability in the inverse problem. The authors are investigating a scheme of allowing the inverse system to adjust the given modal data during the nonlinear iterations.

Acknowledgment

The second author appreciates the financial support from the Korea Research Foundation (KRF-2002-041-D00101).

References

[1]Vanderplaats, G. N., "Structural Optimization," *AIAA Journal*, Vol. 20, No. 7, 1982, pp. 992–1000.

[2]Rao, S. S., *Engineering Optimization, Theory and Practice*, Wiley, New York, 1996, Chap. 1.

[3]Kim, K. O., Anderson, W. J., and Sandstrom, R. E., "Nonlinear Inverse Perturbation Method in Dynamic Analysis," *AIAA Journal*, Vol. 21, No. 9, 1983, pp. 1310–1316.

[4]Moeller, P. W., and Friberg, O., "Updating Large Finite Element Models in Structural Dynamics," *AIAA Journal*, Vol. 36, No. 10, 1998, pp. 1861–1868.

[5]Cherki, A., Lallenmand, B., Tison, T., and Level, P., "Improvement of Analytical Model Using Uncertain Test Data," *AIAA Journal*, Vol. 37, No. 4, 1999, pp. 489–495.

[6]Kammer, D. C., "Sensor Placement for On-Orbit Modal Identification and Correlation of Large Space Structures," *Journal of Guidance, Control, and Dynamics*, Vol. 14, No. 2, 1991, pp. 251–259.

[7]Cobb, R. G., and Liebst, B. S., "Sensor Placement and Structural Damage Identification from Minimal Sensor Information," *AIAA Journal*, Vol. 35, No. 2, 1997, pp. 369–374.

[8]James, G., Zimmerman, D., and Cao, T., "Development of a Coupled Approach for Structural Damage Detection with Incomplete Measurements," *AIAA Journal*, Vol. 36, No. 12, 1998, pp. 2209–2217.

[9]Berman, A., "Multiple Acceptable Solutions in Structural Model," *AIAA Journal*, Vol. 33, No. 5, 1995, pp. 924–927.

[10]Friswell, M. I., and Mottershead, J. E., *Finite Element Model Updating in Structural Dynamics*, Kluwer Academic, Norwell, MA, 1995, Chaps. 1–3.

[11]Friswell, M. I., Penny, J. E. T., and Garvey, S. D., "Parameter Subset Selection in Damage Location," *Inverse Problems in Engineering*, Vol. 5, No. 3, 1997, pp. 189–215.

[12]Penny, J. E. T., Friswell, M. I., and Garvey, S. D., "Automatic Choice of Measurement Locations for Dynamic Testing," *AIAA Journal*, Vol. 32, No. 2, 1994, pp. 407–414.

[13]Meirovitch, L., *Fundamentals of Vibrations*, McGraw–Hill, New York, 2001, pp. 331–333.

[14]Friswell, M. I., and Penny, J. E. T., "Is Damage Location Using Vibration Measurements Practical?," *EUROMECH 365 International Workshop: DAMAS 97, Structural Damage Assessment Using Advanced Signal Processing Procedures*, European Mechanics Society, Sheffield, England, U.K., 1997, pp. 351–362.

[15]Bathe, K. J., *Finite Element Procedures*, Prentice–Hall, Upper Saddle River, NJ, 1996, pp. 844–845.

[16]Guyan, R. J., "Reduction of Stiffness and Mass Matrices," *AIAA Journal*, Vol. 3, No. 2, 1965, p. 380.

[17]Friswell, M. I., Garvey, S. D., and Penny, J. E. T., "Using Iterated IRS Model Reduction Techniques to Calculate Eigensolutions," *Proceedings of the 15th International Modal Analysis Conference*, Society for Experimental Mechanics, Bethel, CT, 1997, pp. 1537–1543.

[18]Zhang, D. W., and Li, S., "Succession-Level Approximate Reduction (SAR) Technique for Structural Dynamic Model," *Proceedings of the 13th International Modal Analysis Conference*, Society for Experimental Mechanics, Bethel, CT, 1995, pp. 435–441.

[19]Kim, K. O., and Kang, M. K., "Convergence Acceleration of Iterative Modal Reduction Methods," *AIAA Journal*, Vol. 39, No. 1, 2001, pp. 134–140.

[20]O'Callahan, J., Avitabile, P., and Riemer, R., "System Equivalent Reduction Expansion Process (SEREP)," *Proceedings of the 7th International Modal Analysis Conference*, Society for Experimental Mechanics, Bethel, CT, 1989, pp. 29–37.

[21]Papadopoulos, M., and Garcia, E., "Improvement in Model Reduction Schemes Using the System Equivalent Reduction Expansion Process," *AIAA Journal*, Vol. 34, No. 10, 1996, pp. 2217–2219.

[22]Papadopoulos, M., and Garcia, E., "Sensor Placement Methodologies for Dynamic Testing," *AIAA Journal*, Vol. 36, No. 2, 1998, pp. 256–263.

S. Saigal
Associate Editor